

Size dependence of the blocking temperatures and electron magnetic resonance spectra in NiO nanoparticles

H. Shim^a, P. Dutta^a, M.S. Seehra^{a,*}, J. Bonevich^b

^aDepartment of Physics, West Virginia University, Morgantown, WV 26506-6315, United States

^bNational Institute of Standards and Technology, Gaithersburg, MD 20899, United States

Received 18 October 2007; accepted 20 October 2007 by A.H. MacDonald

Available online 26 October 2007

Abstract

Size dependence of the blocking temperature T_B (determined by SQUID magnetometry) and electron magnetic resonance (EMR) spectra are reported for NiO nanoparticles (NPs) with diameter $D = 5\text{--}20$ nm. Comparison of the T_B vs. D variations in the oleic acid (OA) coated and uncoated NiO NPs is made. The higher blocking temperatures observed for the uncoated NPs are suggested to result from the effects of the interparticles interactions (IPI). For the coated NPs with negligible IPI, the expected linear variation of T_B with volume V of the NPs is valid if effective anisotropy constant K_{eff} increases with decreasing V . The decreasing intensity of the EMR signal with increasing D is suggested to result from the surface Ni^{2+} spins whose density decreases with increasing D .

© 2007 Elsevier Ltd. All rights reserved.

PACS: 75.50Tt; 75.20.-g; 75.50.Ee; 76.50.+g

Keywords: A. Magnetic nanoparticles; B. Blocking temperatures; C. Size dependence; D. Electron magnetic resonance

Antiferromagnets with their magnetic ordering or Néel temperature T_N higher than 300 K are attractive candidates for applications in spin-valve devices [1]. Bulk NiO, a type-2 antiferromagnet with the NaCl crystal structure, is one such system with $T_N = 523$ K [2]. Below its T_N , magnetic ordering in bulk NiO consists of Ni^{2+} moments parallel in the (111) plane with the adjoining (111) planes ordered antiferromagnetically so that the total magnetization in zero magnetic field is zero [2]. Neutron scattering [3] and magnetic susceptibility (χ) studies [4] revealed a large spin reduction $\Delta S = 0.19$ from the expected $S = 1$ state of Ni^{2+} .

With decrease in particle size (D) of antiferromagnets (AF) to nm dimensions, the effect of surface spins with their lower coordination and broken exchange bonds, and whose concentration increases as $1/D$, often leads to uncompensated moments on AF nanoparticles, yielding superparamagnetism and associated interesting properties. An important characteristic feature of superparamagnets is their blocking temperature T_B . To explain the observed large H_c (coercivity), H_{eb}

(exchange-bias) and μ_p (magnetic moment/particle) in NiO NP below T_B , Kodama et al. [5] via modelling predicted multi-sublattice spin states involving four or even eight sublattices for sizes $D < 7$ nm. These multisublattice states results from low coordination of the surface sites whereas the threshold size ~ 7 nm is strongly dependent on the surface roughness and broken-bond density [5]. However, to date, direct observation of such ordering through neutron scattering has not yet been reported. A recent paper by Li et al. [6] reported room temperature nonzero H_c in NiO NP for all sizes less than 50 nm, with maximum of $H_c = 900$ Oe for $D \simeq 20$ nm. These results are in clear contradiction to earlier studies in NiO where blocking temperature $T_B \simeq 200$ K was reported in 5 nm NiO NP [5, 7, 8] and because H_c is expected to be zero for $T > T_B$. Unfortunately, Li et al. [6] did not report any data of T_B or TEM morphology on their samples although their results imply that T_B for all their samples is above room temperature.

For noninteracting NP of volume V and anisotropy K , the Néel–Brown model for superparamagnetic relaxation yields [9]

$$kT_B = KV/\ell n(f_o/f_m). \quad (1)$$

* Corresponding author.

E-mail address: mseehra@wvu.edu (M.S. Seehra).

Table 1

The summary of the particle sizes calculated from TEM analysis, comparing the results obtained from the XRD measurements for the uncoated NiO NPs

Annealing temperature T_a (K)	TEM (rods)		Calculated effective D (rods) (nm)	TEM (Sphere) Diameter (nm)	XRD (nm) (uncoated)
	Diameter (nm)	Length (nm)			
523	1.7 ± 0.5	25 ± 8	4.8 ± 1.4	5 ± 1	5 ± 0.4
573	2.0 ± 0.7	20 ± 5	4.9 ± 1.5	7 ± 2	7 ± 1.4
623	3.0 ± 0.8	20 ± 5	6.5 ± 1.7	9 ± 2	8 ± 2.0
673	–	–	–	13 ± 3	12 ± 1.1
723	–	–	–	16 ± 3	16 ± 1.2
773	–	–	–	23 ± 5	20 ± 1.5

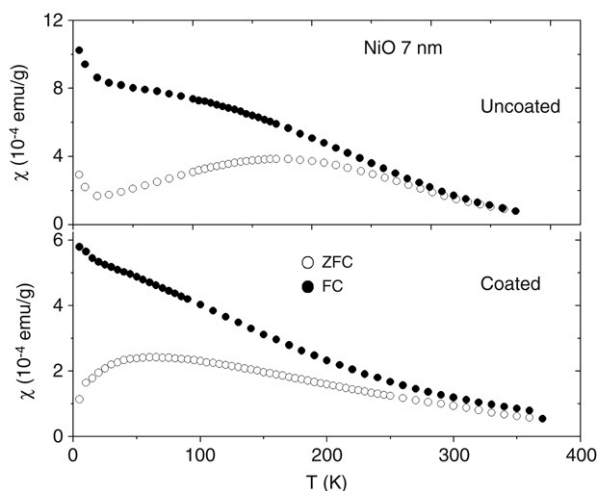


Fig. 1. Magnetic susceptibility χ vs. temperature plots for the 7 nm coated and uncoated NiO in the zero field-cooled (ZFC) and field-cooled (FC) cases.

Here k is the Boltzmann constant, f_o is the attempt frequency and f_m is the frequency of measurements for T_B . The linear variation of T_B with V predicted by Eq. (1) has been reported for noninteracting ferritin NP although a non-zero T_B was inferred in the limit $V = 0$ [10]. For weaker interparticle interactions (IPI) represented by effective temperature T_o , T_B is enhanced by T_o i.e. $T_B = T_o + [KV/k\ln(f_o/f_m)]$, a result based on the Vogel–Fulcher relaxation [11]. The data in ferrofluids [11] and in uncoated 5 nm NiO NP [12] have been well fitted to this equation with T_o increasing with the strength of the IPI. With decrease in size D of NP, K may increase and becomes size-dependent because of additional contributions from surface anisotropy [13], thus breaking down the linearity of T_B to V Eq. (1) even in the absence of IPI.

In this paper, we report our results on the size dependence of T_B and electron magnetic resonance (EMR) spectra in NiO NP of sizes 5–20 nm. Measurements are reported for the uncoated as well as oleic acid (OA) coated NP, the latter with negligible IPI as shown later. Our results suggest that in NiO NP, size dependent magnetic anisotropy and IPI play important roles in the observed magnetism of NiO NP as size D is varied. Recent results of Winkler et al. [14] on 3 nm NiO NP and those of Tiwari et al. [15] on 5, 6, and 8 nm NiO NP are also included in our discussion of the results.

Our procedures used for synthesizing NiO NP are similar to those used by others [7,8,15] and involve annealing Ni(OH)₂ gel at temperatures $T_a = 523$ –773 K to yield particles of average size (diameter) D from 5 nm to 20 nm respectively.

Transmission electron microscopy (TEM) and Scherrer relation in x-ray diffraction (XRD) were used to characterize size and morphology of the NPs. Temperature variations of the magnetization M were measured with a commercial SQUID magnetometer and EMR data were taken with a standard X-band spectrometer operating at 9.28 GHz.

The sizes determined by TEM and XRD for the uncoated NPs obtained by annealing at $T_a = 523$, 573, 623, 673, 723 and 773 K are summarized in Table 1. Only lines due to NiO are observed in XRD. In TEM, we measured about 40 particles in the micrographs to tabulate the data of Table 1. For the lower T_a , some of the particles are in the form of nanorods [8,16] of length ℓ and diameter d while others have rounded morphology. For nanorods, we used the volume $V = \pi d^2 \ell / 4 = \pi D^3 / 6$ to determine the effective size D of a sphere of equivalent volume with the corresponding equation for the uncertainty $\delta D / D = 2\delta d / 3d + \delta \ell / 3\ell$. The results of Table 1 show that, within the uncertainties, the effective diameters of the nanorods are in good agreement with the diameters of the rounded particles for the same T_a . Similar procedures were used for the OA coated NPs. To produce the OA coated NPs, we followed the procedure used by Bodker et al. [17].

For the OA-coated and uncoated 7 nm NiO NPs, the data of χ vs. T for the zero field-cooled (ZFC) and field-cooled (FC) cases are shown in Fig. 1 as a representative data for all sizes. The average blocking temperature T_B defined by peak in χ (ZFC) is 170 K (55 K) for the uncoated (coated) 7 nm NP. Results of similar measurements for other sizes are plotted as T_B vs. size D in Fig. 2, including the data of Makhlof et al. for 5 nm uncoated NP [7], Winkler et al. for 3 nm highly-diluted NP [14], Tiwari et al. for uncoated 5, 6 and 8 nm NP [15], and Bodker et al. for 5 nm uncoated and OA-coated NiO NP [17]. Winkler et al. [14] diluted their 3 nm NiO NP down to 0.55% concentration in polyvinyl-pyrrolidone to reduce IPI. The fact that our data and that of Bodker et al. on OA coated NP fall in line with that of Winkler et al. [14] for the diluted sample suggests that IPI in the OA-coated NiO NP are also negligible. Data from references [7,15] and [17] for uncoated NiO NPs, also plotted in Fig. 2, fit the overall behaviour of increasing T_B with decreasing D for $D < 8$ nm as observed in our samples. The consistency of our data for the larger size range in Fig. 2 with the several earlier reports on select sizes [7,14,15,17] provides considerable confidence that the overall pattern of the variation of T_B with size D for the coated and uncoated NiO NPs shown in Fig. 2 is a trustworthy phenomenon. In their studies of the uncoated 5, 6 and 8 nm NiO NPs, Tiwari et al. [15]

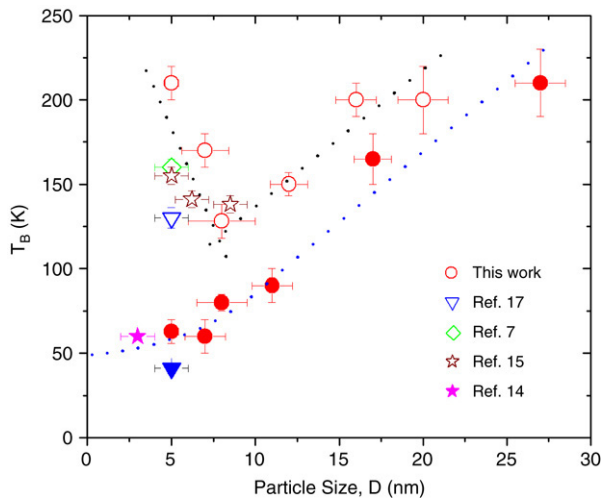


Fig. 2. Variation of the blocking temperature T_B vs. size D of the NiO NP with the open (closed) symbols for the uncoated (coated) NP. The dotted lines are drawn as guides.

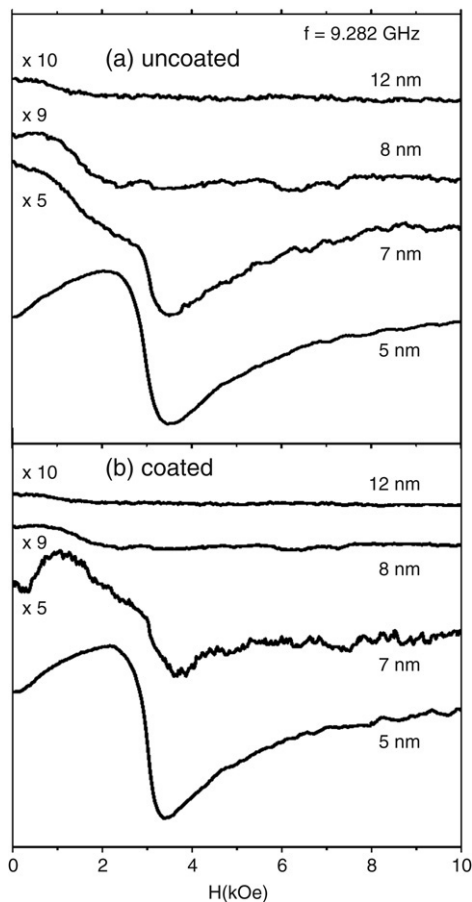


Fig. 3. Derivative EMR spectra at 300 K for the (a) uncoated and (b) OA-coated NiO NPs.

have argued that T_B value of these particles shown in Fig. 2 represent spin-glass like ordering of the surface spins. A similar increase in T_B with decreasing particle size has been reported recently in MnO NPs [18].

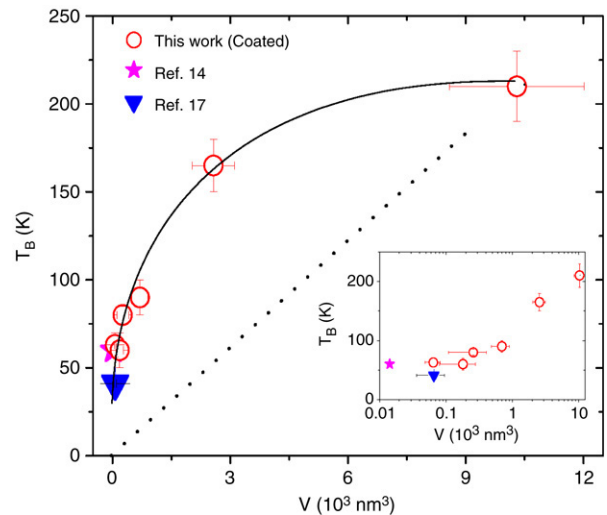


Fig. 4. Plot of blocking temperatures T_B against volume V of the OA-coated NiO NPs. The solid line is drawn using the variation of K_{eff} with V shown in Fig. 5. The inset shows an expanded view of the variation for smaller V . The dotted line is drawn for a constant $K_{\text{eff}} = 0.72 \times 10^5$ ergs/cm³.

The size dependence of the observed EMR spectra at 300 K is shown in Fig. 3(a) for the uncoated and in Fig. 3(b) for the OA-coated NiO NP. The signal intensity decreases rapidly with increase in size so that for $D > 8$ nm, the EMR signal essentially disappears. Temperature dependence of the EMR parameters of the observed signal in our 5 nm NP has been discussed in an earlier paper [8]. A similar EMR study has been reported by Winkler et al. [14] in their 3 nm diluted NiO NP. The noteworthy new result here is the decreasing EMR signal with increase in the particle size.

For the OA-coated and diluted NiO NP, interparticle interactions (IPI) are considered to be negligible as noted earlier. According to Eq. (1) T_B should approach zero as volume V of the nanoparticles approaches zero. To check this, the data of T_B vs. V is plotted in Fig. 4 for the coated/diluted samples in which IPI is expected to be negligible. Since this variation of T_B vs. V is clearly nonlinear, especially for lower V , the solid line is a fit to Eq. (1) using the anisotropy energy K as the fitting parameter (labelled here as K_{eff}). The plot of K_{eff} vs. V used for drawing the solid line in Fig. 4 is shown in Fig. 5. Obviously K_{eff} increases with decreasing volume and hence size D of the NiO NP. This analysis also shows that $T_B \rightarrow 0$ as $V \rightarrow 0$ cannot be ruled by the data of Fig. 4. If $K_{\text{eff}} = 0.72 \times 10^5$ ergs/cm³ for the largest V in Fig. 4 is used and it did not increase with decreasing D , then the dotted curve shown in Fig. 4 would result, clearly in disagreement with the experiments. In the NPs of Fe and Fe₃O₄ [13], an increase in K_{eff} with decreasing D has been attributed to the surface anisotropy in the smaller NP so that $K_{\text{eff}} = K_b + (6/D)K_s$ where K_b is the anisotropy constant for bulk and K_s is the surface anisotropy constant [13]. In NiO NP, K_{eff} does increase with decrease in D but it does not quite fit the $1/D$ variation (inset of Fig. 5) except for the smaller D for which the morphology is more rod-like (Table 1). Using theoretical/modelling studies, Yanes et al. [19] have shown in a recent study that the above $1/D$ variation is valid only for

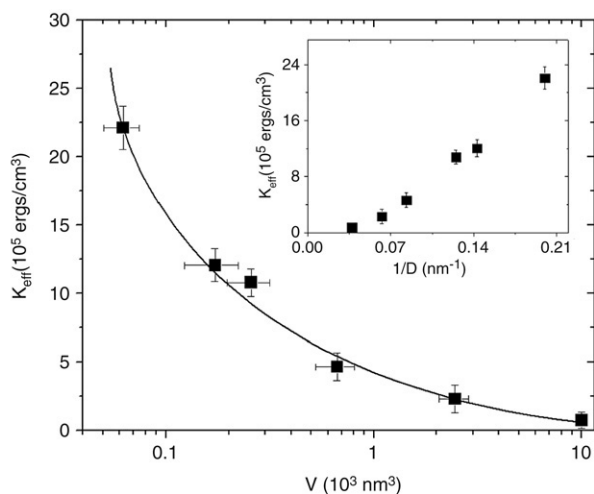


Fig. 5. Variation of K_{eff} with volume V of the coated NiO NPs derived from the fit to the data in Fig. 4. In the inset, the nonlinear variation of K_{eff} with $1/D$ is evident.

elongated (nanorod) particles and not for spherical (rounded) particles. Our results in Fig. 5 seem to confirm this.

For the uncoated NP with particles in close proximity to one another, IPI can be quite significant especially since the magnetic moment per particle $\mu_p = 1250\mu_B$ for the 5 nm NiO NP is quite large [8]. The dipole–dipole interaction energy considering only z nearest neighbours is approximately equal to $z\mu_p^2/r^3$. Using $r = 5$ nm, $z = 6$ and $\mu_p = 1250\mu_B$ yields 47 K as the magnitude of this energy in temperature units. For $\mu_p = 2000\mu_B$ estimated by Makhlof et al. [7] in their 5.3 nm NiO NP, similar analysis yields 100 K as the estimate for IPI. From the fit of the measured T_B with f_m (the frequency of measurements), $T_o = 162$ K (derived from the Vogel-Fulcher relaxation mentioned earlier) was determined for the 5 nm uncoated NiO NP as the contribution to T_B from IPI, with T_o being zero for the OA-coated NiO NP [12]. Considering that even the short-range interparticle exchange-interaction, which was not included in the above calculations, could become significant if the particles are packed densely and are in contact, and we have ignored the effect of distant neighbours, the above crude estimates of $T_o = 47$ K and 100 K for the 5 nm NiO NP are quite satisfactory in comparison to the experimental value of $T_o = 162$ K [12]. A number of modelling studies on the effects of dipole–dipole interaction on T_B have been reported [20], all showing increase in T_B measured by magnetometry due to IPI in densely packed NP. Since the average separation between the particles increases with increase in size and μ_p decreases [5], this contribution should decrease with increasing D as observed experimentally in Fig. 2.

The decrease of the intensity of EMR signal with increase in the particle size for both the coated and uncoated particles is in line with the fact that bulk NiO is EMR silent. For the Ni^{2+} spins on the surface of the NPs, two facts are valid: (i) the fraction of the surface spins to the total number of spins/particle decreases with size D as m/D , m being determined by the morphology of the NP; and (ii) the surface Ni^{2+} are relatively weakly-coupled to the interior spins and they are relatively “free” spins. Both of these facts along with the experimental

results of Fig. 3 lead us to suggest that the observed EMR signal is due to the weakly-coupled surface Ni^{2+} spins. The strong intensity of the EMR signal near $g = 2$ for the smallest particles (Fig. 3) may be due to the fact the morphology factor m is nearly 60% larger for the nanorod dimensions shown in Table 1 as compared to spherical particles of equivalent volume. The coincidence of the observation of the EMR signal and the predicted multisublattice spin structure for $D < 8$ nm [5] may be fortuitous.

In summary, we have presented T_B vs. diameter D and volume V behavior of the uncoated and coated NiO NPs and shown that our data (and those of others on select sizes) present a consistent picture. For the coated NPs in which the interparticle interactions (IPI) are negligible, T_B follows the linear variation with V if the anisotropy constant increases with decrease in volume as expected. For the uncoated particles, T_B is larger and increases with decreases in D for $D < 8$ nm due to the additional effects of increasing IPI, in line with modeling studies [20]. The observed decrease in the intensity of EMR signal with increasing size is understandable if the EMR signal is due to the uncompensated surface Ni^{2+} spins. A more rigorous theoretical interpretation of the variation of K_{eff} with size of the NiO NPs is warranted.

Acknowledgement

The research at West Virginia University was supported in part by the US Department of Energy, contract #DE-FC26-05NT42456.

References

- [1] R.L. Stamps, J. Phys. D: Appl. Phys. 33 (2000) R247; J. Nogués, I.K. Schuller, J. Magn. Magn. Mater. 192 (1999) 203.
- [2] W.L. Roth, J. Appl. Phys. 31 (1960) 2000. And references therein.
- [3] H.A. Alperin, J. Phys. Soc. Jpn. 17-B3 (1962) 12.
- [4] G. Srinivasan, M.S. Seehra, Phys. Rev. B 29 (1984) 6295.
- [5] R.H. Kodama, S.A. Makhlof, A.E. Berkowitz, Phys. Rev. Lett. 79 (1997) 1393; R.H. Kodama, A.E. Berkowitz, Phys. Rev. B 59 (1999) 6321.
- [6] L. Li, L. Chen, R. Qihe, G. Li, Appl. Phys. Lett. 89 (2006) 134102.
- [7] S.A. Makhlof, F.T. Parker, F.E. Spada, A.E. Berkowitz, J. Appl. Phys. 81 (1997) 5561.
- [8] M.S. Seehra, P. Dutta, H. Shim, A. Manivannan, Solid State Commun. 129 (2004) 721.
- [9] L. Néel, Ann. Geophys. 5 (1949) 99; W.F. Brown, Phys. Rev. 130 (1963) 1677.
- [10] S. Gider, D.D. Awschalom, T. Douglas, S. Mann, M. Chaparala, Science 268 (1995) 77.
- [11] J. Zhang, C. Boyd, W. Luo, Phys. Rev. Lett. 77 (1996) 390.
- [12] H. Shim, A. Manivannan, M.S. Seehra, K.M. Reddy, A. Punnoose, J. Appl. Phys. 99 (2006) 08Q503.
- [13] K. Gilmore, Y.U. Idzerda, M.T. Klem, M. Allen, T. Douglas, M. Young, J. Appl. Phys. 97 (2005) 10B301; F. Bodker, S. Morup, S. Linderorth, Phys. Rev. Lett. 72 (1994) 282.
- [14] E. Winkler, R.D. Zysler, M.V. Mansilla, D. Fiorani, Phys. Rev. B 72 (2005) 132409.
- [15] S.D. Tiwari, K.P. Rajeev, Phys. Rev. B 72 (2005) 104433.
- [16] M.S. Seehra, H. Shim, P. Dutta, A. Manivannan, J. Bonevich, J. Appl. Phys. 97 (2005) 10J509.
- [17] F. Bodker, M.F. Hansen, C.B. Koch, S. Morup, J. Magn. Magn. Mater. 221 (2000) 32.

- [18] A. Morales, R. Skomski, S. Fritz, G. Shelburne, J.E. Shield, M. Yin, S. O'Brien, D.L. Leslie-Pelecky, Phys. Rev. B 75 (2007) 134423.
- [19] R. Yanes, O. Chubykalo-Fesenko, H. Kachkachi, D.A. Garanin, R. Evans, R.W. Chantrell, Phys. Rev. B 76 (2007) 064416.
- [20] J.L. Dormann, L. Bessais, D. Fiorani, J. Phys. C. 21 (1988) 2015;
- R.W. Chantrell, N. Walmsley, J. Gore, M. Maylin, Phys. Rev. B 63 (2000) 024410;
- D. Kechrakos, K.N. Trohidu, Phys. Rev. B 58 (1998) 12169;
- P. Allia, et al., Phys. Rev. B 64 (2001) 144420;
- S. Morup, Europhys. Lett. 28 (1994) 671.